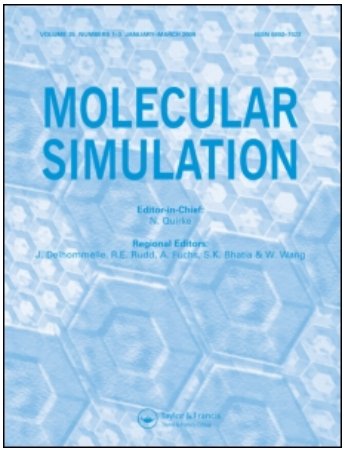


**Molecular Simulation**
Publication details, including instructions for authors and subscription information:
http://www.informaworld.com/smpp/title~content=t713644482

# The Effect of Molecular Geometry on Boundary Layer Lubrication

Y. C. Kong[ab]; D. J. Tildesley[ac]
[a] Department of Chemistry, University of Southampton, Southampton [b] Computational Dynamics Ltd., London [c] Unileuv Research, Mersegside

**To cite this Article** Kong, Y. C. and Tildesley, D. J.(1999) 'The Effect of Molecular Geometry on Boundary Layer Lubrication', Molecular Simulation, 22: 2, 149 — 168
**To link to this Article: DOI:** 10.1080/08927029908022092
**URL:** http://dx.doi.org/10.1080/08927029908022092

*Molecular Simulation*, 1999, Vol. 22, pp. 149–168
Reprints available directly from the publisher
Photocopying permitted by license only



# THE EFFECT OF MOLECULAR GEOMETRY ON BOUNDARY LAYER LUBRICATION

Y. C. KONG* and D. J. TILDESLEY**

*Department of Chemistry, University of Southampton, Southampton S017 1BJ*

*(Received April 1998; accepted April 1998)*



Simulation studies of the friction between layers of dialkyl surfactants have been performed using a non-equilibrium molecular dynamics method. The model layers at a temperature of 298 K and a normal pressure of 210 MPa are sheared at a relative velocity of $1\,ms^{-1}$. The friction coefficient has been studied as a function of the molecular geometry by simulating bilayers of $C_{10}C_{18}$ (asymmetrical) and $C_{18}C_{18}$ and $C_{10}C_{10}$ (symmetrical) surfactants. In all cases the hydrocarbon chains are attached to a positively charged dimethylammonium head-group which interacts with a negatively charged surface. At a head-group area of 50 $Å^2$ per molecule, the friction between the layers of asymmetrical surfactants is greater than that between layers of symmetrical surfactants at approximately the same normal pressure. At 77 $Å^2$ the friction between the $C_{18}C_{10}$ layers remains higher than that of the $C_{18}C_{18}$ layers but is now lower than that of the $C_{10}C_{10}$, where the surface structure is highly disordered and the two layers are separated by only 15.8 Å. The friction between the layers correlates well with the amount of layer overlap as defined by the common area under the chain density profiles. These observation, which are in broad aggreement with the experimental measurement on similar di-chain surfactants are rationalised in terms of the translational, orientational and conformational structures of the layers.

*Keywords:* Non-equilibrium; molecular dynamics; boundary layer lubrication; dialkyl surfactants

## 1. INTRODUCTION

Molecularly thin films of organic molecules play a key role in the boundary layer lubrication of solid surfaces [1–7]. A detailed understanding of the structure and dynamics of surfactant bilayers in a parallel slit geometry

*Present address: Computational Dynamics Ltd., Olympic House, 317 Latimer Road, London W10 6RA.

**Corresponding author. At Unileuv Research, Quarry Road East, Bebington, Wirral, Mersegside L63 35w.

provides a simple model of the lubrication process and allows us to study the effects of surface density, chain length, temperature, shearing velocity and contact pressure on interlayer friction. These simulations are the first step in building molecular models of technologically important processes such as adhesion, lubrication, wear, fabric softening, and conditioning [8–14].

In this paper, we consider cationic surfactants of the dialkyl quaternary ammonium family (*e.g.*, dioctadecyldimethylammonium chloride (DODAC)). In aqueous solution, positively charged liposomal particles composed of these surfactant molecules are attracted to the negatively charged cotton surface. As the surface of the fabric drys, the surfactant molecules spread rapidly from the air–water–particle, three-phase contact line across the air–water interface to form a well ordered Langmuir film. Finally the surfactant molecules are transferred as a Langmuir-Blodgett film to the fabric surface [15]. It is our contention that some understanding of the conditioning process can be gained by studying the behaviour of the well-ordered monolayer physically adsorbed to a surface moving past a second adsorbed surfactant layer.



Experiments on the lubrication of DODAC films have been performed by Chugg and Chaudri using a sliding spherical stylus on film-coated, flat substrates [16, 17]. These experiments can elucidate the effect of contact pressure, the number of friction cycles, the substrate temperature and the sliding velocity on the friction coefficient. In a non-equilibrium molecular dynamics simulation, we can attempt to model the friction coefficient directly. Two films are sheared in the opposite direct at a constant positive normal pressure and constant relative sliding velocity. The average force, $\langle F_x \rangle$ in the direction of the shear is measured over a period of nanoseconds. The friction coefficient, $\mu$, is simply

$$\mu = \frac{-\langle F_x \rangle}{\langle F_z \rangle} \tag{1}$$

where $\langle F_z \rangle$ is the average normal force [18, 19]. Thus, in principle, we can understand the detailed molecular structural changes in the bilayer that give rise to changes in the friction.

In a previous paper, describing simulations of DODAC bilayers [20], we demonstrated that a non-equilibrium molecular dynamics method could be used to estimate the friction coefficient between layers of surfactant molecules adsorbed on a surface. Using a parallel molecular dynamics code, we performed simulation at shearing velocities of between 1 and 100 $\mathrm{ms}^{-1}$ of systems at head-group areas per molecule of 50 and 77 $\mathrm{\AA}^2$. The

head-group area or the area per surfactant molecule is the inverse of the surface number density. For the system at 50 $Å^2$ and 1 $ms^{-1}$ the simulated friction coefficient is 0.15 compared to the extrapolated experimental value of 0.11. We observed that the friction coefficient: decreased with increasing normal force; increased with decreasing surfactant density; and increased with increasing shearing velocity.

During the shearing process, the strong electrostatic interactions between the charged head-groups and the counter-ions attached to the surface meant that there was little slip between the layer and the wall. The ordered hexagonal structure of the counter-ions induced a solid head-group structure but even at high coverage, the radial distribution of the methyl tail groups was liquid-like. At all of the shearing velocities studied in this paper, the surfactants align with the direction of the flow.

In the present paper, we study the effect of surfactant architecture on the molecular structures and friction coefficient. Bilayer simulations are performed on the surfactants, dioctadecyl-dimethyl-ammonium chloride, $C_{18}C_{18}$, decyl-octadecyl-dimethyl ammonium chloride, $C_{10}C_{18}$, and didecyl-dimethyl ammonium chloride $C_{10}C_{10}$. The layer are sheared with a relative shearing velocity is 1 $ms^{-1}$. The $C_{10}C_{18}$ surfactant is chosen as an example of a bilayer which is expected to exhibit a molecularly rough interface. Unlike the mixed monolayers formed from single chain $C_{18}$ and $C_{10}$ surfactants there is no opportunity for the phase separation in which the long and the short chains demix in the layer. These simulations were performed at two different surfactant head-group areas to study the effect of the coverage on friction.

The paper is organised as follows: in Section 2 we provide a brief account of the potential model and the simulation method. Section 3 contains a discussion of our results obtained for different geometries and converges and Section 4 contains our conclusions.

## 2. MODEL AND SIMULATION

The model of the dioctadecyldimethylammonium chloride has been described in detail elsewhere [21]. Briefly, the bond-lengths are fixed at their equilibrium values using constraint dynamics implemented within the SHAKE algorithm. The three-atom valence angle distortions are controlled using the normal harmonic potential. The three torsional potentials, CCCC, CCCN and CCNC, are described by potentials of the form used by Rykaert and Bellemans for butane [22].

The non-bonded interactions between atoms in the same molecule that are separated by at least atoms along the contour of the surfactant are modelled using a Lennard-Jones potential with a cut-off of 2.5 $\sigma_{MeMe} = 8.82$ Å. All atoms in different molecules interact through the same Lennard-Jones potential. The methylene and methyl groups in the hydrocarbon chains are treated as anisotropic united atoms using the method of Toxvaerd [23]. For these united atoms, the force sites are displaced from the centre of the carbon atom along the bisector of the HCH bond angle in the CCC plane.

The unit positive charge on the head-group is represented by four charges of $0.25|e|$ placed on the carbon atoms alpha to the nitrogen [24]. This is balanced by a charge of $-1|e|$ on the counter ion. The charge–charge interactions are calculated using the Ewald-like method of Hautman and Klein [25]. This method is designed for systems which have a quasi-two-dimensional periodicity.

Each of up to forty sites in a surfactant interact with the surface through the usual 9–3 integrated Lennard-Jones potential, which depends only on the height of the site above the surface. The surface density, $\rho = 0.142$ Å$^{-3}$, required for this potential is derived from the crystal structure of cellulose, since cotton is one of the substrates of interest. In the real system, the positively charged head-groups interacts with the negatively charged phenolic groups on the surface of the cotton and the chlorine associated with the head group is washed away with the counterions from the surface. The amphiphile is physically adsorbed onto the surface by a strong electrostatic interaction between the head-group and a negative surface residue. In these simulations the negative ions are fixed in an hexagonal array at a height of $z = 3$ Å from the zero of the 9–3 potential. These surface ions consist of a full negative charge with a Lennard-Jones repulsion dispersion potential. They move with the surface during the shear sustaining their two-dimensional structure and exerting a strong, attractive force on the ammonium cations.

The full details of the parameters used in this paper are contained in Table II of [21] with the RB dihedral potential and without the image charge interactions. A sketch of the initial configuration of the simulations for the $C_{10}C_{18}$ system is shown in Figure 1. The initial configuration of the amphiphiles in one layer was taken from a production simulation of the monolayer. A copy of this configuration was rotated through 180° and placed directly above the first layer at a suface separation of approximately 80 Å. The two surfaces were moved towards one another in the $z$-direction until the required contact pressure is achieved. The separation of the

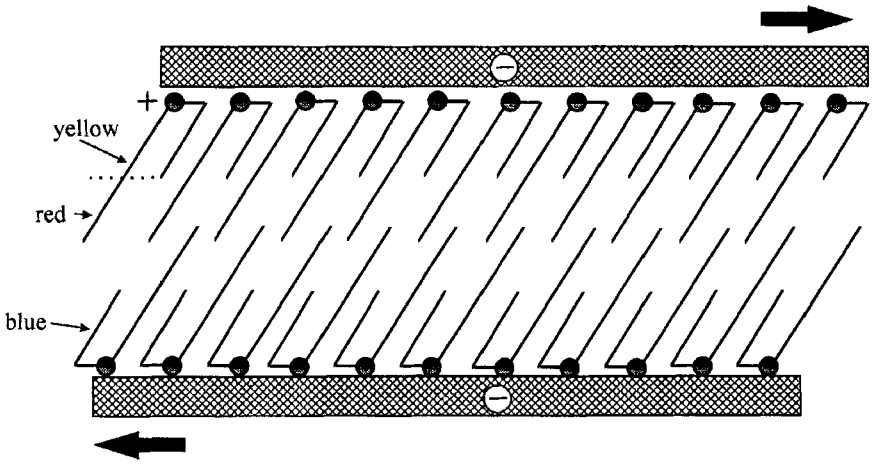


FIGURE 1 A sketch of the starting geometry in the bilayer configuration. Each positive charge on the amphiphile is balanced by a corresponding negative charge attached to the surface ensuring that the overall layer is electrically neutral. The colours refer to those used in Figure 3(a).



surfaces can be adjusted manually during the course of the simulation or the surfaces can be moved towards one another steadily at a pre-chosen rate. The $C_{10}C_{18}$ bilayers were prepared by truncating the hydrocarbon chain with gauche defect in each $C_{18}C_{18}$ chain and pushing the two walls together to achieve the required normal pressure. In a similar way, the $C_{10}C_{10}$ bilayers were obtained by truncating both octadecyl chains.

At a head-group area of $57\,\text{Å}^2\,\text{molecule}^{-1}$ the $C_{18}C_{18}$ layers form a structure where the amphiphiles are tilted at an angle of 45° to the surface normal in which one of the chains in the amphiphile sustains a $\{g^+g^+tg^+g^+\}$ conformational defect close to the head-group which allows it to bend around and follow in the direction of the second all trans chain. The combination of the conformational defect and the tilt means that a layer of the symmetrical surfactants $C_{18}C_{18}$ and $C_{10}C_{10}$ produce a flat surface for the next layer to pack against. A defect of this type must exist in the layered structure of the dialkyl quaternary ammonium salts to create a reasonable intramolecular structure to allow for efficient in-plane packing.

The two layers are sheared in opposite direction along the box-fixed $x$-axis by moving the counterions in layers a distance

$$\Delta x = \pm \frac{v_x \delta t}{2}. \tag{2}$$

at each time-step, where $\delta t = 2.5 \times 10^{-15}$ s and $v_x$ is the relative sliding velocity. The layer is initially sheared in the direction orthogonal to the molecular tilt. During the course of the simulation the heat is removed from the system using a uniform thermostat and all of the runs are performed close to room temperature. In determining the current temperature, the drift velocity in the $x$-direction is determined separately for both layers

$$v_{x,\text{drift}} = \frac{\sum_i (m_i v_{ix})}{\sum_i m_i} \tag{3}$$

The kinetic energy of the system is determined with the calculated drift velocity adjustment applied to the molecules in each layer:

$$KE = \frac{1}{2} \sum_i m_i [(v_{ix} - v_{x,\text{drift}})^2 + v_y^2 + v_z^2] \tag{4}$$

The current molecular temperature is evaluated from $(3N - N_c)kT/2 = KE$ where $N_c$ is the total number of constraints in the system. The temperature is reduced to the required value ($T = 298.15$ K) by rescaling the molecular velocities. In particular in the direction of the shear.

$$v_{ix,\text{new}} = v_{ix} \sqrt{T/T_{\text{current}}} + v_{x,\text{current,drift}} \tag{5}$$

Finally, the constraint algorithm is applied to obtain the present coordinates using the old coordinates, the current forces and the new rescaled velocities.

The details of the replicated-data parallelisation of the molecular dynamics code and its implementation on a number of shared memory and distributed memory parallel machines is reported in [26].

## 3. RESULTS AND DISCUSSIONS

The $C_{18}C_{18}$, $C_{10}C_{18}$ and $C_{10}C_{10}$ dialkyldimethylammonium chloride bilayer simulations were performed at 298.15 K and fixed wall separations at a shearing velocity of 1 $ms^{-1}$. These simulations were designed to investigate the effect of structure of the surfactants on their efficiency as lubricants. The effect of other variables such as shearing velocity on the symmetrical surfactants have been reported elsewhere [20].

For the three different surfactants, the normal pressure was changed by pushing the walls slowly together in order to achieve a value of approximately 210 MPa. Instead of using discontinuous step changes in the

wall separation followed by a equilibration of 100000 to 200000 steps, it was found to be more effective to dynamically adjust the separation at a velocity of $1\,ms^{-1}$ (*i.e.*, 0.1 Å per 4000 steps). This gradual movement of the walls induces smaller perturbation to the interlayer forces and the corresponding oscillations in the normal pressure are significantly smaller. A final shorter equilibration phase of between 40000 to 80000 time-steps follows the adjustment to the separation.

A summary of the simulations performed in this study is given in Table I. Runs of between 0.5 and $1.0 \times 10^6$ time-steps were performed to calculate the average structural and thermodynamic properties. We define the overlap of the chains by calculating the common area under the density profiles of both layers (*e.g.*, the shaded area in Fig. 5(a)). Figure 2 shows a plot of the friction coefficient against chain overlap at a normal pressure of $210 \pm 10$ MPa and shearing velocity of $1\,ms^{-1}$ for a number of different surfactants and different surface densities. As reported previously [20], we find a reasonable correlation between the friction coefficient and the chain overlap for the symmetrical surfactants. In these systems the overlap between the layers increases with decreasing surface density at the same normal pressure. For the asymmetrical surfactant, there is a small decrease in chain overlap with decreasing density and the same correlation between friction and overlap. These observations can be rationalised in terms of the different packing at the interface and we will return to this point when we consider the detailed structure of the layers.

The general behaviour of these systems can be illustrated using representative snapshots of the layers taken at the end of the production phase of the simulation. Figure 3(a) shows a snapshot of the $C_{10}C_{18}$ bilayer at a head-group area of $50\,Å^2$ and a shearing velocity of $1\,ms^{-1}$ after 500000 time-steps. The white spheres are the nitrogen atoms of the head-group, the blue lines represents bonds of the $C_{10}$ chain and the last 8 atoms in the $C_{18}$ chain are joined by red lines. Although there is a significant interaction between the $C_{18}$ chains, it is clear that there is no direct repulsive

TABLE I Details of the six molecular dynamics simulations

| *Chain* | $A_m/Å^2$ | $z/Å$ | *No. of timesteps* | *Chain density overlap*/$Å^2$ | $p_{zz}/MPa$ | $\mu$ |
|---|---|---|---|---|---|---|
| $C_{18}C_{18}$ | 50 | 41.0 | 1000000 | 0.005 | 215 | 0.149 |
| $C_{10}C_{18}$ | 50 | 34.0 | 550000 | 0.044 | 219 | 0.310 |
| $C_{10}C_{10}$ | 50 | 26.5 | 544000 | 0.012 | 212 | 0.150 |
| $C_{18}C_{18}$ | 77 | 26.5 | 1000000 | 0.038 | 213 | 0.200 |
| $C_{10}C_{18}$ | 77 | 21.05 | 588000 | 0.040 | 222 | 0.256 |
| $C_{10}C_{10}$ | 77 | 15.8 | 545000 | 0.034 | 206 | 0.272 |

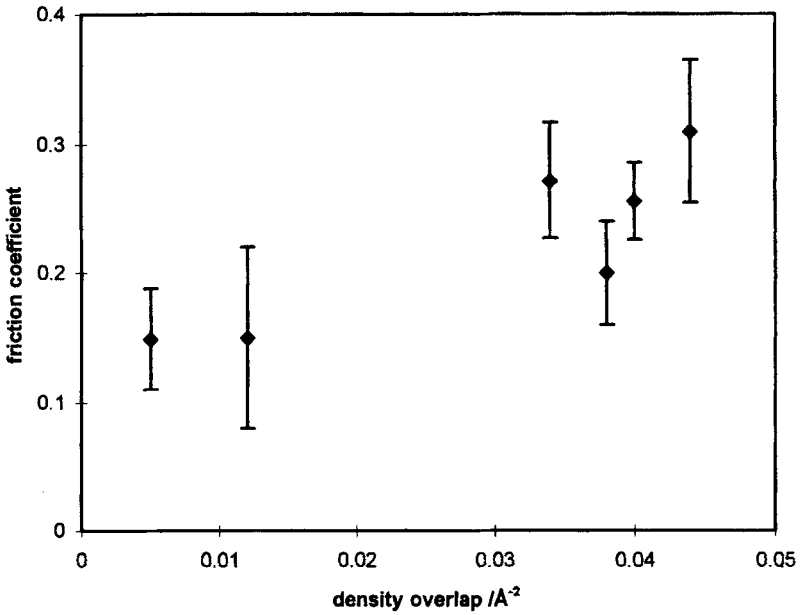


FIGURE 2 A plot of the friction coefficient against chain overlap at a normal pressure of $210 \pm 10$ MPa and shearing velocity of 1 ms$^{-1}$ for a number different surfactants.



interactions between the $C_{10}$ chains of the two layers. The all-trans length of a $C_{18}$ chain is about 8 Å and the combined length of two $C_{10}$ chains and the head-group size is not sufficient for the $C_{10}$ chains to touch at a wall separation of 34 Å. In the interface region, the $C_{18}$ chains are inter-digitated at the required normal pressure and the chain tails exhibits a "liquid-like" structure. As a result of this overlap, the friction coefficient of the $C_{10}C_{18}$ system is significantly larger compared with dialkyldimethylammonium cationic surfactants with chains of equal lengths at the same normal pressure, coverage and shearing velocity.

In the 77 Å$^2$ head-group area system, the wall separation distance of 21.05 Å is required to obtain a normal pressure of 210 MPa and this separation is small enough to allow both the $C_{10}$ and $C_{18}$ chains to be in contact (Fig. 3(b)). At this surface density and pressure both chains are present at the interface leading to a more efficient packing and less interdigitation between the layers. This results in a smaller overlap and a lower friction coefficient. The friction coefficient decreases with decreasing head-group area for the $C_{10}C_{18}$ bilayer in contrast with the behaviour of the $C_{18}C_{18}$ and $C_{10}C_{10}$ systems.

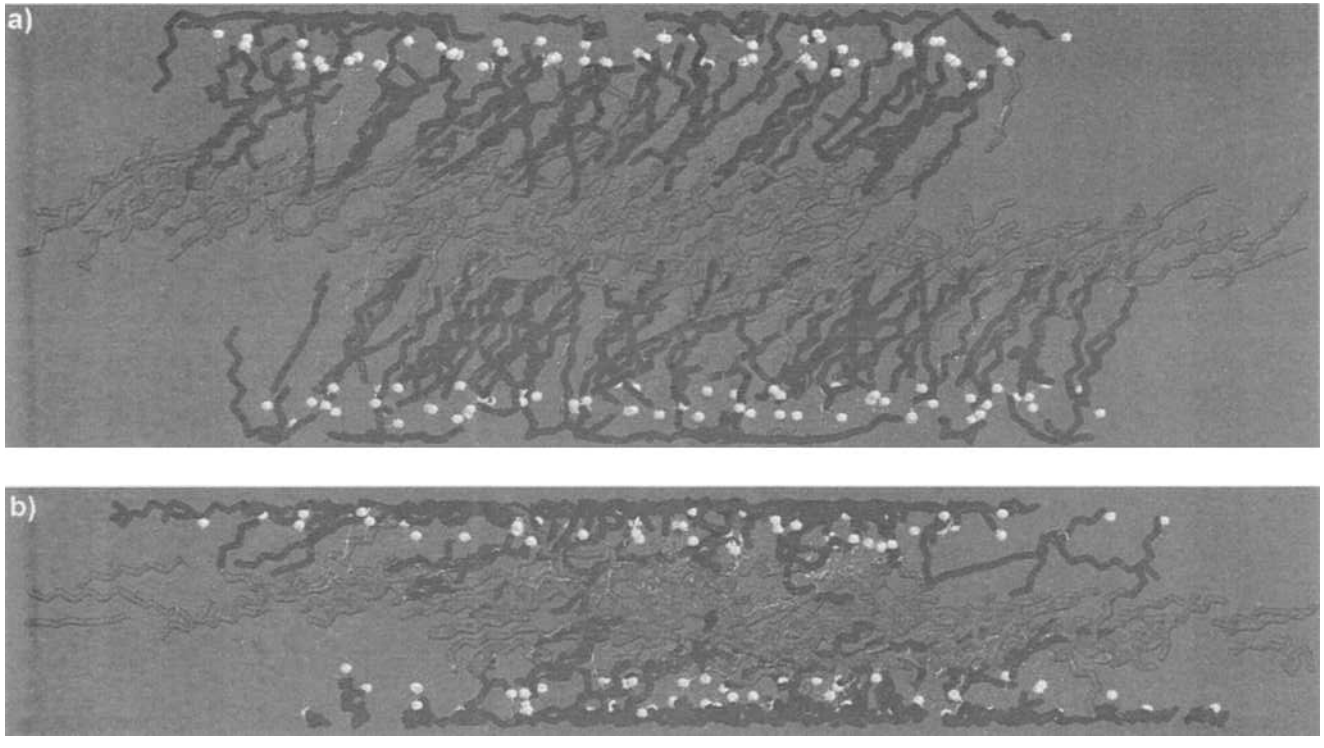


FIGURE 3 Snapshots of the $C_{10}C_{18}$ bilayer at a normal pressure of $210 \pm 10$ MPa and 298.15 K after shearing at 1 $ms^{-1}$ for 500000 time-steps. The white spheres are the nitrogen atoms of the head-group, the blue lines represents bonds of the $C_{10}$ chain and the last 8 atoms in the $C_{18}$ chain are joined by red lines: a) 50 $Å^2$ $molecule^{-1}$; b) 77 $Å^2$ $molecule^{-1}$. (See Color Plate I).

The differences between the asymmetrical and symmetrical surfactants can be most clearly seen by comparing the representative structures shown in Figures 3 and 4. Figure 4 shows typical configurations from the $C_{18}C_{18}$ and $C_{10}C_{10}$ bilayers at head-group areas of 50 and 77 $Å^2$ and a pressure of 210 MPa. The colour scheme is different from that used in Figure 3. The last 8 atoms of the chains are joined by blue lines in the upper layer and by red lines in the lower to enable us to focus on the interface. The surfactant interface is clearly defined at a head-group area of 50 $Å^2$ and the surfactants

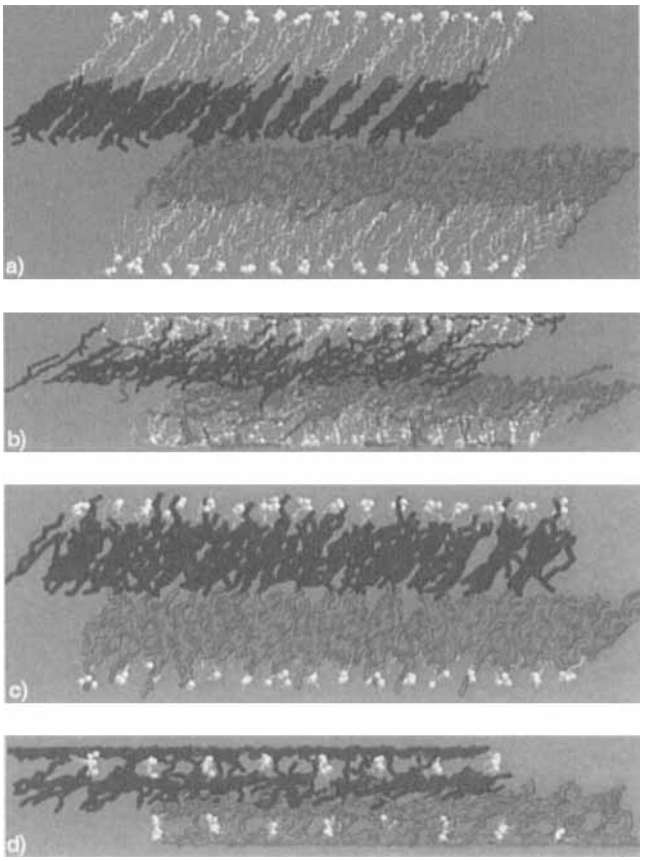


FIGURE 4 Snapshots of the $C_{18}C_{18}$ and $C_{10}C_{10}$ bilayers at a normal pressure of $210 \pm 10$ MPa and 298.15 K after shearing at 1 ms $^{-1}$ for 1000000 and 500000 time-steps respectively. The final 8 atoms of the chains are joined by blue lines for the upper and red for the lower layer: a) $C_{18}C_{18}$ bilayer with head-group area of 50 $Å^2$; b) $C_{18}C_{18}$ bilayer with head-group area of 77 $Å^2$; c) $C_{10}C_{10}$ bilayer with head-group area of 50 $Å^2$; d) $C_{10}C_{10}$ bilayer with head-group area of 77 $Å^2$. (See Color Plate II).

exhibit a "solid-like" structure with clear translational order particularly at the base of the chains. When the head-group area is increased to 77 Å$^2$, the chain tails become conformationally disorders or more "liquid-like" and the overlap between the two layers increases leading to a higher friction coefficient. The contrast between Figure 3(a) and Figures 4(a) and (d) at the same surface coverage is marked.

The qualitative observaions suggested by the snap-shots are supported by the average structural distribution functions calculated from averages over the complete trajectories. Figure 5(a) shows the chain number density profile of the $C_{10}C_{18}$ bilayer at 50 Å$^2$. The chain density profile, which excludes the head group atom, consists of a small peak near each wall, corresponding to the atoms of the hydrocarbon chain that have adsorbed onto the surface. Figure 3(a) suggests that this adsorption is mainly due to the shorter $C_{10}$ chains. There is also a broad, featureless region corresponding to the conformationally disordered or liquid-like hydrocarbon chains that exist away from the wall. There are slight asymmetries in the profiles that result from the slow relaxation in the surface regions. The $C_{10}C_{18}$ profile is significantly



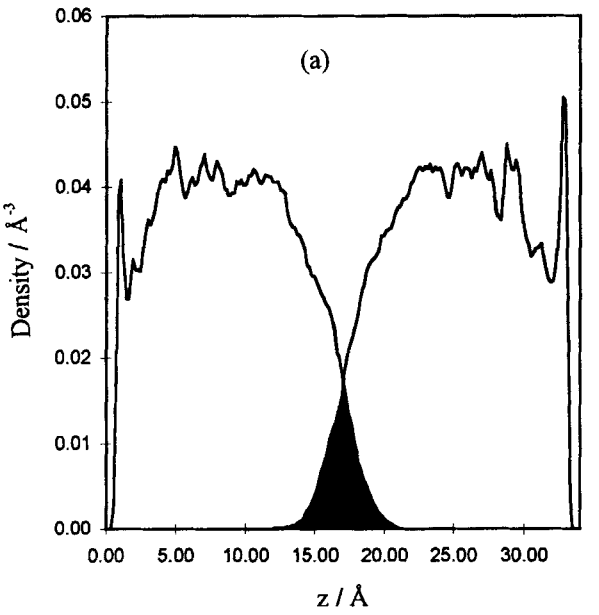


FIGURE 5 The chain number density profile for the $C_{10}C_{18}$ bilayer at a normal pressure of 210 ± 10 MPa and 298.15 K after shearing at 1 ms$^{-1}$ for 500000 time-steps: a) $A_m$ = 50 Å$^2$, $z$ = 34 Å; b) $A_m$ = 77 Å$^2$, $z$ = 21.05 Å. The hatched region indicates the extent of the chain overlap.

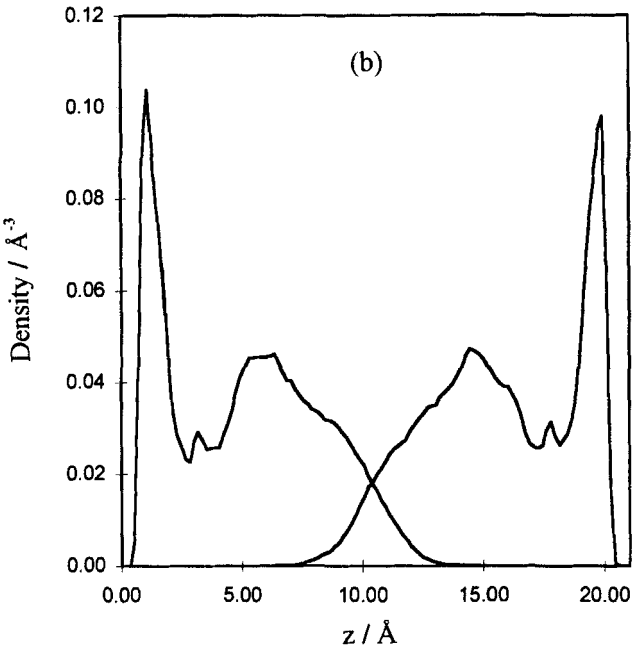


FIGURE 5 (Continued).



different from that exhibited by the $C_{18}C_{18}$ surfactant at the same conditions. In this case $\rho(z)$ for each layer exhibits nine clearly resolvable peaks and a much smaller overlap region (The actual density profiles for the symmetrical surfactants have appeared elsewhere; see Figure 6(a) of [20], and we do not reproduce them here.). Figure 5(b) shows the profile for the $C_{10}C_{18}$ system at a higher head-group area of 77 Å$^2$; this corresponds to a lower surface density or a surfactant with a larger head-group. This profile exhibits sharp peaks at the walls which are characteristic of strong adsorption of hydrocarbon chains onto the surfaces that occur under the shear. The profile is almost identical in structure to that of the $C_{18}C_{18}$ system at the same area per molecule (see Fig. 7 of [20]). The chain density profiles of the $C_{10}C_{10}$ bilayer at a head-group area of 50 Å$^2$ and 77 Å$^2$ have the same structures as those of the corresponding $C_{18}C_{18}$ bilayer.

The nitrogen or *head-group* density profiles for the $C_{10}C_{18}$ system are shown in Figure 6. Figure 6(a) shows the nitrogen number density of the $C_{10}C_{18}$ system at a head-group area of 50 Å$^2$. The peak is split into a doublet with sharp features at approximately 3 Å and 4.4 Å from the adsorbing wall. (These are average values from both profiles). This is in contrast to the head-

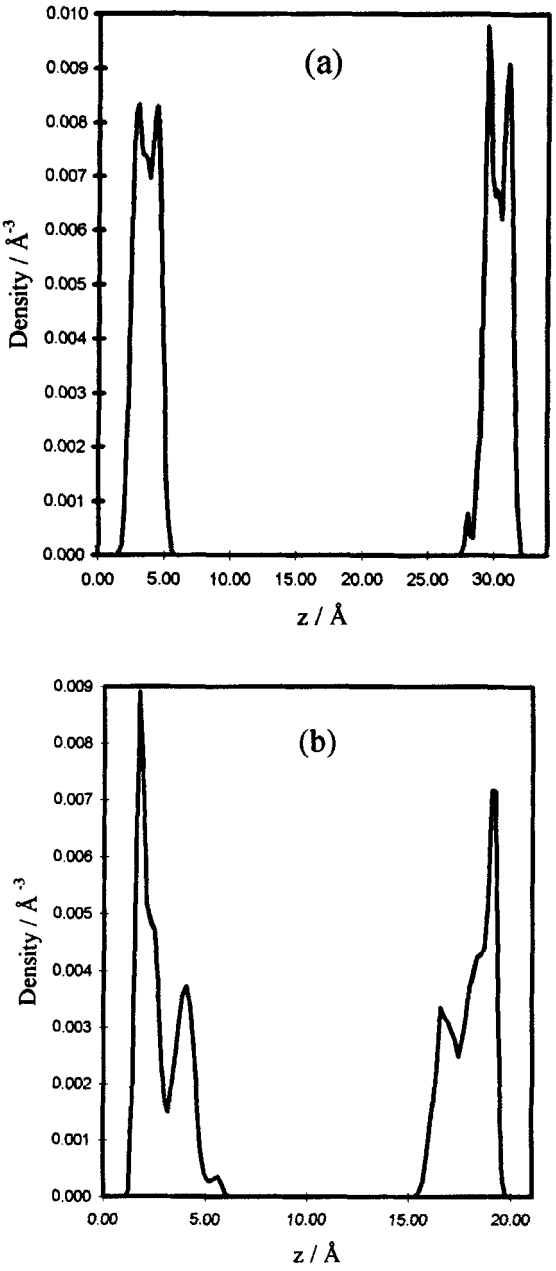


FIGURE 6 The nitrogen or head-group number density profile of the $C_{10}C_{18}$ bilayer at a normal pressure of $210 \pm 10$ MPa and 298.15 K after shearing at 1 ms$^{-1}$ for 500000 time-steps: a) $A_m = 50$ Å$^2$, $z = 34$ Å; b) $A_m = 77$ Å$^2$, $z = 21.05$ Å.

group density profiles for the symmetrical systems that exhibit **one** sharp peak with the nitrogen at 3 Å from the wall. There are clear indications of this bi-modal behaviour in the snapshot shown in Figure 3(a). There are two reasonable explanations for a shift of the head-group: (a) the gain in inter-layer dispersion energy obtained by pulling the $C_{10}$ chain into the bilayer interface; (b) the gain in intra-layer dispersion energy obtained by efficiently aligning longer sections of the $C_{10}$ and $C_{18}$ chains in the same surfactant. These gains are off-set by the loss of the attractive electrostatic interactions between the head-group cation and the surface anions and by the loss of the dispersion energy associated with the chain–surface interaction. Structurally, both mechanisms (a) and (b) can be achieved by movements that attempt to equalise the two chain lengths; that is by moving the $C_{10}$ chain closer to the bilayer interface, pulling the head-group further from the wall and allowing the surfactant to pivot around some point in the longer $C_{18}$ chain. A sketch representing this idea is shown in Figure 7. It is clear from $\rho_H(z)$ at 50 Å$^2$ that not all of the head-groups leave the surface, approximately half the nitrogen atoms are strongly adsorbed It is difficult to understand why the distribution is bimodal rather than a continuous decay from a maximum at $z = 3$ Å. It may be that pivot point of the chain moves a fixed number of $CH_2$ links along the $C_{18}$ branch shifting the nitrogen atom

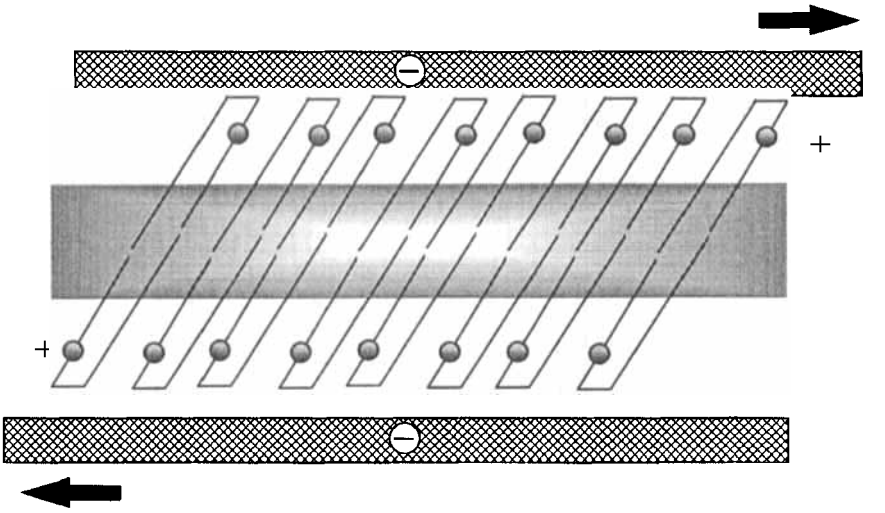


FIGURE 7 The chain equalisation mechanism postulated for the $C_{10}C_{18}$ bilayer system. The shaded area indicates the region of increased attractive interlayer and intralayer dispersion interactions.

up by 1.4 Å. Further shifts might be prevented by the strong electrostatic interaction between the anions and cations; this would explain the precise positions of the peaks but not the equal distribution. We can offer no simple explanation for this. At 77 $Å^2$, $\rho_H(z)$ is slightly broader and has two more clearly defined peaks that are separated by an average distance of 2.3 Å. The first peak is pushed closer to the surface by the normal pressure to an average distance of 1.9 Å.

The disorder in the head-group structure for the $C_{10}C_{18}$ system is confirmed by the in-plane radial distribution function of the nitrogen atoms. Figure 8 shows $g(r)$ for the $C_{10}C_{18}$ and $C_{18}C_{18}$ bilayers at 50 $Å^2$. The solid line is the result for the symmetrical surfactant and this shows six clear peaks associated with an almost perfect triangular lattice. The head-group structure is strongly correlated with the lattice of anions in the surface. The $g(r)$ for the $C_{10}C_{18}$ is more disordered but not liquid-like. Although the



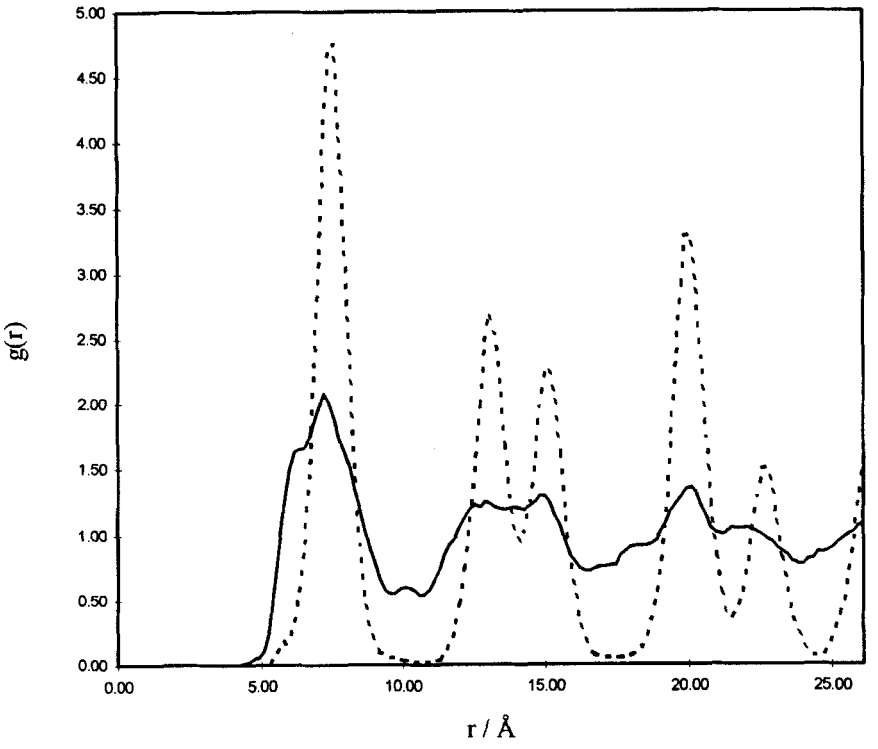


FIGURE 8 The nitrogen in-plane radial distributions of the $C_{10}C_{18}$ and $C_{18}C_{18}$ bilayer at a normal pressure of 210 ± 10 MPa and 298.15 K after shearing at 1 $ms^{-1}$ for 500000 and 1000000 time-steps. The solid line represents the mixed chain and the dashed line the equal chain length system.

first peak height is reduced from 4.7 to 2, there are still clear signs of a double second peak and the third peak of the triangular structure. The $g(r)$ for the $C_{10}C_{18}$ system would be typical of a glassy state with some medium range translational order. The surfactants do not diffuse in the surface plane.

The tilt of the surfactants can be calculated from the instantaneous moment of inertia tensor of each surfactant in the space-fixed system. The tensor is diagonalised and the principal axes determined from the eigenvector associated with the smallest eigenvalue. The cosine of the angle between this axis and the surface normal ($z$-axis) is used to construct the tilt distribution $n(\cos\theta)$. A crude measure of the layer orientation is the mean tilt, $\bar{\theta} = \cos^{-1}(\overline{n(\cos\theta)})$. $\bar{\theta}$ for the $C_{10}C_{18}$ bilayers at of the 50 Å$^2$ and 77 Å$^2$ systems is 40° and 53° respectively (The corresponding tilts in the $C_{18}C_{18}$ systems are 45° and 60°. Both systems exhibit a broad distribution around these mean values. At both densities the chains align in the direction of the shear.

Figures 9(a) and (b) show the chain torsional distribution of the $C_{10}C_{18}$ at head-group areas of 50 Å$^2$ and 77 Å$^2$ respectively. The torsional angles

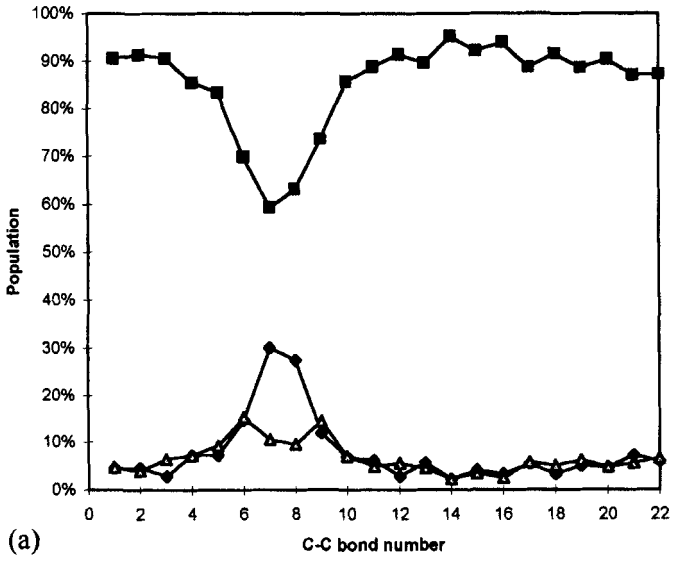


FIGURE 9 The amphiphile torsional angles of the $C_{10}C_{18}$ bilayer at a normal pressure of $210 \pm 10$ MPa and 298.15 K after shearing at 1 ms$^{-1}$ for 500000 time-steps. The $C_{10}$ and $C_{18}$ torsions are given by the angles 1–7 and 8–22 respectively. The trans conformation is ■■■ and the gauche conformations ◆◆◆ and ▲▲▲; a) $A_m = 50$ Å$^2$, $z = 34$ Å; b) $A_m = 77$ Å$^2$, $z = 21.05$ Å.

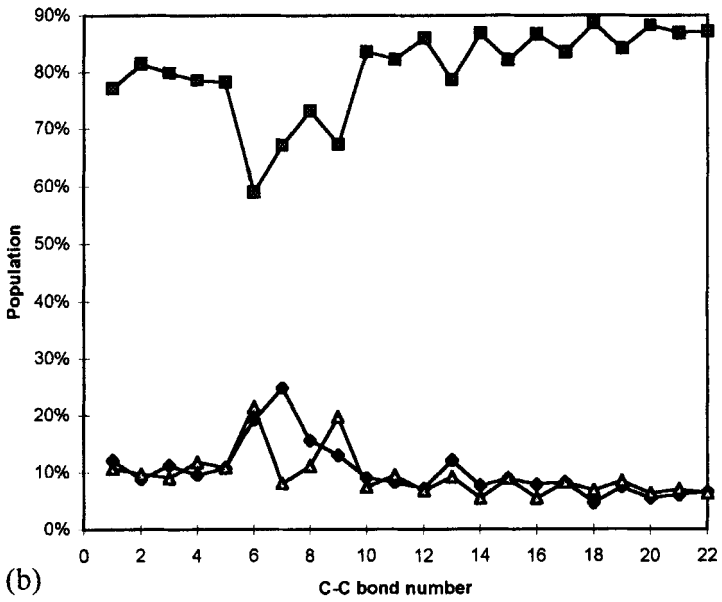


FIGURE 9 (Continued).

involving four carbon atoms in the shorter $C_{10}$ chain are labelled 1–7 in moving from the free end of the chain to the nitrogen head-group. For the longer $C_{18}$ chain these torsions are labelled 8–22 moving from the head-group to the free end of the chain. The percentage of dihedral angle is the trans conformation (IUPAC standard conformations $\varphi = 180 \pm 60°$) is shown as squares and the percentage of gauche conformations ($60 \pm 60°$ and $300 \pm 60°$) by the diamonds ($g^+$) and triangles ($g^-$). The chain torsional distribution of the $C_{10}C_{18}$ and $C_{10}C_{10}$ bilayers are similar in shape to those of the $C_{18}C_{18}$ system but the asymmetrical chain system has a higher proportion of gauche conformations along the whole length of the chain. The $C_{10}C_{18}$ system at 50 Å$^2$ has approximately 10% of the conformational degrees of freedom in gauche states with a slightly higher frequency in the $C_{18}$ than $C_{10}$ chains. In the 77 Å$^2$ head-group are for the $C_{10}C_{18}$ system, this rises to 20% and 15% for the $C_{10}$ and $C_{18}$ chains respectively. Figure 9(a), shows that the kink ($g^+g^+tg^-g^-$) localised in the shorter chain at the start of the simulation has been delocalised over both the $C_{10}$ and $C_{18}$ chains (centred at C—C bond numbers 7 and 8 respectively). In all three systems the kink is delocalised around the C—C bonds closest to the nitrogen atom of the head-group. This delocalisation of this defect is greater for the $C_{10}C_{10}$ chain and smaller in the $C_{18}C_{18}$ systems and is consistent with the movement

of the $C_{10}$ chain towards the surfactant interface. In the layer at 77 $Å^2$ (Fig. 9(b)) the gauche defects in the hydrocarbon chain are more uniform distributed across all the torsions for the three different surfactants.

## 4. CONCLUSION

In this paper, we have simulated the friction coefficient between two surfactant layers composed of $C_{10}$ and $C_{18}$ chains grafted to the same head-group (an asymmetrical surfactant). This friction coefficient is compared to those calculated for the $C_{18}C_{18}$ and $C_{10}C_{10}$ bilayers (symmetrical surfactants) at approximately the same normal pressure. At a head-group area of 50 $Å^2$ per molecule, the friction between the layers of asymmetrical surfactants is greater than that between layers of symmetrical surfactants. At 77 $Å^2$ the friction between the $C_{18}C_{10}$ layers remains higher than that of the $C_{18}C_{18}$ layers but is now lower than that of the $C_{10}C_{10}$ where the surface structure is highly disordered and the two layers separated by only 15.8 Å. The friction between the layers correlates well with the amount of layer overlap as defined in terms of the chain density profiles.

These results can be rationalised in terms of the average structure of the surfactant layers. A Langmuir-Bloggett monolayer of a dialkyldimethyl-ammonium cationic surfactant with equal chain lengths forms a regular interface with a vacuum. If a bilayer is constructed by bringing two of these regular monolayers together at 50 $Å^2$, the chain tails form a sharp interface with the surfactants in a solid-like structure, resulting in a low friction coefficient. When a monolayer is constructed from surfactants consisting of chains of different lengths, it would be expected to form a surface with longer chain protruding in a regular fashion from the denser base of the layer. For a bilayer of these asymmetrical surfactants, there is significant interlayer digitation of the free surfactant chain ends resulting in a higher friction coefficient at the same normal pressure.

Chugg [16, 17] has carried out similar experiments on the effect of chain length on the friction coefficient between two surfaces coated with a single monolayer of dialkyldimethylammonium salts at constant normal pressure of 206 MPa and shearing velocity of 0.1 $mms^{-1}$. The series of measurements on the surfactants, $C_{18}C_{18}$, $C_{18}$ Ph and $C_{12}C_{12}$, allow the most direct comparison with our simulations. The friction coefficient of $C_{18}C_{18}$, $C_{18}$ Ph and $C_{12}C_{12}$ are 0.05, 0.10 and 0.07 respectively. The $C_{12}C_{12}$ is representative of the shorter chain $C_{10}C_{10}$ system our simulation. It should be noted that the mixed chain

$C_{18}$ Ph system is different from our $C_{10}C_{18}$ system in two ways: firstly the head-group area is slightly lower than 50 $Å^2$ and secondly the phenyl group is smaller and more rigid than the $C_{10}$ chain. Nevertheless, the general results of the model are in agreement with experiment with a significantly higher friction coefficient for the asymmetrical surfactant. The fact that the overall magnitude of the experimental friction coefficients is smaller that those simulated can be understood in part by the difference in the simulated and experimental shearing velocities. Our previous work indicates a significant decrease in the overall friction coefficient with decreasing shearing velocity [20].

We predict that the two types of layers will behave differently if the surface density is decreased. For the layers formed from the symmetrical surfactants, decreasing the packing density results in a significant loss of translational and conformational order and a corresponding increase in the overlap of the layers. The friction coefficient increases with decreasing surface density. For the asymmetrical surfactants, the additional space near the head-group allow for significant structural rearrangements with the $C_{10}$ chains moving into the surfactant interface creating a denser more closely packed interfacial structure. This contrast with the large spaces or voids left in the contact layer at 50 $Å^2$. The overall friction coefficient is reduced with decreasing surface density in this case.



### *Acknowledgements*

DJT would like to thank the EPSRC for a grant GR/K83878 for computing resources. YCK would like to thank the Consortium for MPP Supercomputing in Materials Chemistry for a generous allocation of computer time on the Edinburgh Cray T3D/512.

### *References*

[1] Yoshizawa, H., Chen, Y.-L. and Israelachvili, J. (1993). "Fundamental mechanisms of interfacial friction.1. Relation between adhesion and friction", *J. Phys. Chem.*, **97**, 4128.
[2] Yoshizawa, H. and Israelachvili, J. (1993). "Fundamental mechanisms of interfacial friction.2. Stickslip friction of spherical and chain molecules", *J. Phys. Chem.*, **97**, 11300.
[3] Thompson, P. A. and Robbins, M. O. (1990). "Origin of stick-slip motion in boundary lubrication", *Science*, **250**, 792.
[4] Schmitt, V., Lequeux, F., Pousse, A. and Roux, D. (1994). "Flow behaviour and shear-induced transition near an isotropic-nematic transition in equilibrium polymers", *Langmuir*, **10**, 955.
[5] Gee, M. L., McGuiggan, P. M., Israelachvili, J. and Homola, A. M. (1990). "Liquid to solid-like transitions of molecularly thin-films under shear", *J. Chem. Phys.*, **93**, 1895.
[6] Horn, R. G., Hirz, S. J., Hadziioannou, G., Frank, C. W. and Catala, J. M. (1989). "A revaluation of forces measured across thin polymer-films-nonequilibrium and pinning effects", *J. Chem. Phys.*, **90**, 6767.

[7] Klein, J., Kumacheva, E., Mahalu, D., Perahia, D. and Fetters, L. J. (1994). "Reduction of frictional forces between solid-surfaces bearing polymer brushes", *Nature*, **370**, 634.
[8] Horn, R. G., Israelachivili, J. and Pribac, F. (1987). "Measurement of the deformation and adhesion of solids in contact", *J. Coll. Interf. Sci.*, **115**, 480.
[9] Landman, U., Leudtke, W. D., Burnham, N. A. and Colton, R. J. (1990). "Atomistic mechanisms and dynamics of adhesion, nanoindentation, and fracture", *Science*, **248**, 4954.
[10] Landman, U., Luedtke, D. and Ringer, E. M. (1992). "Atomistic mechanisms of adhesive contact formation and interfacial processes", *Wear*, **153**, 3.
[11] Smith, J. R., Bozzolo, G., Banerjea, A. and Ferrante, L. (1989). "Avalanche in adhesion", *Phys. Rev. Lett.*, **63**, 1269.
[12] Sebastian, S. A. R. D., Bailey, A. I., Briscoe, B. J. and Tabor, D. (1986). "Effect of a softening agent on yarn pull-out force of a plain weave fabric", *Text Res. J.*, **56**, 604.
[13] Rabinowicz, E. (1965). Friction and Wear of Materials, Wiley, New York.
[14] Cohen, S. R., Neubauer, G. and McClelland, G. M. (1990). "Nanomechanics of a au-ir contact using a bidirectional atomic force microscope", *J. Vac. Sci. & Technol. A*, **8**, 3449.
[15] Jones, C. C. (1993). Private communication, Unilever Port Sunlight Research Laboratory.
[16] Chugg, K. J. (1990). *Ph.D. Thesis*, St Edmunds College, Cambridge.
[17] Chugg, K. J. and Munawar Chaudri, M. J. (1993). "Boundary lubrication and shear properties of thin solid films of dioctadecyl dimethyl ammonium-chloride (TA100)", *Phys. D. Appl. Phys.*, **26**, 1993.
[18] Glosli, J. N. and McClelland, G. M. (1993). "Molecular-dynamics study of sliding friction of ordered organic monolayers", *Phys. Rev. Lett.*, **70**, 1960.
[19] Harrison, J. A., White, C. T., Colton, R. J. and Brenner, D. (1993). "Effects of chemically-bound flexible hydrocarbon species on the frictional-properties of diamond surfaces", *J. Phys. Chem.*, **97**, 6573.
[20] Kong, Y. C. and Tildesley, D. J. (1997). "The molecular dynamics simulation of boundary layer lubrication", *Molec. Phys.*, **92**, 7.
[21] Adolf, D. B., Tildesley, D. J., Pinches, M. R. S., Kingdon, J. B., Madden, T. and Clark, A. (1995). "Molecular-dynamics simulations of dioctadecyldimethylammonium chloride monolayers", *Langmuir*, **11**, 237.
[22] Ryckaert, J. P. and Bellemans, A. (1975). "Molecular dynamics of liquid alkanes", *Chem. Phys. Letts.*, **30**, 123.
[23] Toxvaerd, S. (1990). "Molecular-dynamics calculation of the equation of state of alkanes", *J. Chem. Phys.*, **93**, 4290.
[24] Jorgensen, W. L. and Gao, J. (1986). "Monte-Carlo simulations of the hydration of ammonium and carboxylate ions", *J. Phys. Chem.*, **90**, 2174.
[25] Hautman, J. and Klein, M. L. (1992). "An Ewald summation method for planar surfaces and interfaces", *Mol. Phys.*, **75**, 379.
[26] Surridge, M., Tildesley, D. J., Kong, Y. C. and Adolf, D. B. (1996). "A parallel molecular-dynamics simulation code for dialkyl cationic surfactants", *Parallel Computing*, **22**, 1053.